# Supplementary Information:

## Unlocking Cryogenic Zinc-ion Batteries with a Glycerol Monoallyl Ether-Modulated Aqueous Electrolyte

Shuang Li,†[a] Yating Wang,†[a] Mengyu Zhu,[a] Danling Chen,[a] Jidao Li,[a] Huicai Wang,[a] Wenjing Cheng,[a] Xinning Liang,[a] Zhengshuai Bai,[a] Shi Chen,[c] Yuxin Tang[a,b] and Yanyan Zhang[a,b*]

a College of Chemical Engineering, Fuzhou University, Fuzhou 350108, China

b Qingyuan Innovation Laboratory, Quanzhou 362801, China

c Institute of Applied Physics and Materials Engineering, University of Macau, Macau 999078, P. R. China

* Corresponding author (email: zyanyan@fzu.edu.cn)

### 1. Experimental Section

#### Materials

All reagents and materials were commercially available and used without further purification. Sodium chloride (NaCl, 99.8%), vanadium pentoxide ($V_2O_5$, 97.0%), zinc trifluoromethanesulfonate ($Zn(OTf)_2$, 98.0%), 3-allyloxy-1,2-propanediol ($C_6H_{12}O_3$), and N-methylpyrrolidone (NMP) were purchased from Aladdin. Polyvinylidene fluoride (PVDF; 99.0%) and Ketjen black (KB) were purchased from Kelude.

#### Preparation of electrolytes

A certain amount of zinc trifluoromethanesulfonate powder, weighed in stoichiometric ratio, was dissolved in deionized water, and fully stirred at room temperature until the solution became clear, resulting in a 2 M $Zn(OTf)_2$ electrolyte, which was named AP-0%. In the above-mentioned 2 M $Zn(OTf)_2$ electrolyte, 10%, 20%, 30% and 40% of deionized water in the solvent was replaced with AP, and the prepared electrolytes were named AP-10%, AP-20%, AP-30% and AP-40%, respectively.

**Preparation of $Na_2V_6O_{16}·3H_2O$**

20.0 g of commercial $V_2O_5$ powder was added to a 300 mL 2 M NaCl solution under vigorous stirring at room temperature. Subsequently, the solution color changed from yellow to brownish after 96 h. The obtained brown product was washed with deionized water and ethanol to remove by-products, and finally dried in an 80 °C electric thermostatic drying oven for 12 h.

**Fabrication of NVO Cathodes**

To prepare the NVO cathodes, NVO powder, KB and PVDF were mixed in a weight ratio of 7:2:1 in N-methyl pyrrolidinone to form a slurry, coated on a Ti foil, and then dried at 80 ℃. The mass loading of NVO on the electrode is approximately 2.4 mg $cm^{-2}$.

**Materials Characterization**

The morphology evolution characterization of zinc deposits on the Zn-metal is characterized by SEM (Verios G4 UC). Then, the grain morphology of the microstructure for Zn foil can be explored. XRD (D/MAX-Ultima) is used to study Zn foils after cycling in different electrolytes (in the range $2\theta$ = 5 - 80°, scanning speed of 8°/min). Samples for XRD testing are prepared as follows: rinsing the recycled electrodes with deionized water, soaking them for 12 h, then drying the electrodes overnight at 50 ℃ in a vacuum drying oven, and finally using tape to remove the glass fiber film remaining on the electrode surface. In situ optical microscopy (OLYMPUS) was used to monitor the dynamic morphological evolution of Zn deposition processes in different electrolytes in real-time. FITR spectroscopy (Nicolet iS50) was used to collect bending and stretching information of functional groups of different electrolytes between 650-4000 $cm^{-1}$. The vibration of various electrolytes was collected by a Raman spectrometer (Invia Reflex) with a 532 nm light source. The freezing points of different hydrogel electrolytes were determined by differential scanning calorimetry (DSC, METTLER TOLEDO).

**Electrochemical measurements**

Electrochemical performance tests were conducted using CR2025 coin cells. A glass fiber separator (Whatman, GF/D) was used as the separator, and AP-0%, AP-10%, AP-20%, AP-30%, and AP-40% were employed as the electrolytes. For Zn||Zn and Zn||Cu cells, two zinc foils or metallic Zn foil with a

thickness of 100 μm and Cu foil were used as two electrodes. All types of cells are tested by NEWARE Battery Test System (CT-4008Tn-5V50mA-HWX, Shenzhen, China). Cyclic voltammetry (CV), chronovoltammetry (CA), linear sweep voltammetry (LSV) and linear polarization tests were performed on the CHI 760e electrochemical workstation. The CV tests and the full cells were carried out with the NVO cathode as the working electrode, a zinc plate as the counter and reference electrode. The CA test was carried out with Zn||Zn symmetric batteries. The LSV tests were carried out with stainless steel foil as the working electrode, zinc foil as the counter and reference electrode. The linear polarization test and cyclic voltammogram test were carried out with zinc foil as the working electrode, Ti foil as the counter and reference electrode. The ion conductivity was tested by SS||SS symmetric batteries.

**Computational Methods**

Calculations were carried out by using the Gaussian 09 program suite based on density functional methods. Geometry optimizations have been calculated at B3LYP/6-31G (d, p) level [1, 2] with DFT-D3 dispersion correction.[3] The vibrational frequencies were also calculated for all the studied structures to ensure that there is no imaginary frequency present, which further confirms that the optimization has converged successfully to the local minima on the potential energy surface (PES). The Gibbs free energy (G) is calculated by the following equation:

$$G = E + E_{ZPE} - TS$$

where EZPE, and TS represent the zero-point energy (ZPE) corrections and entropy contribution, respectively. T is the temperature, which is set to 298.15 K.

**The calculated binding energy**

The binding energies have been calculated for different crystal planes of Zn metal as follows:

$$\Delta E_{binding} = E(total) - \sum_{i} E_{components}$$

## 2. Supporting Figures

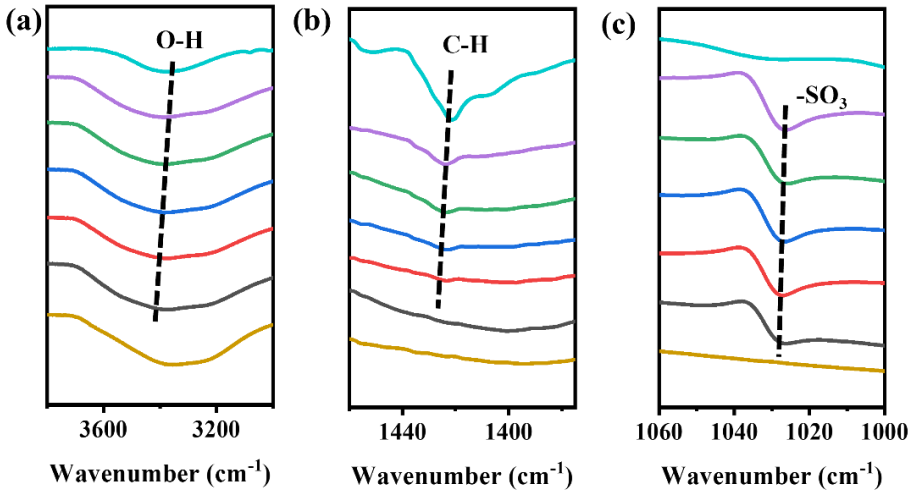


**Figure S1.** FT-IR spectra of different electrolytes.

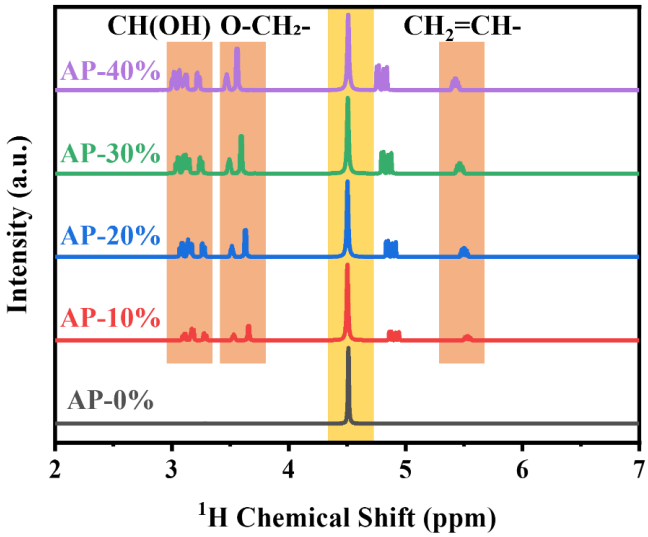


**Figure S2.** $^{1}$H NMR spectra of different electrolytes.

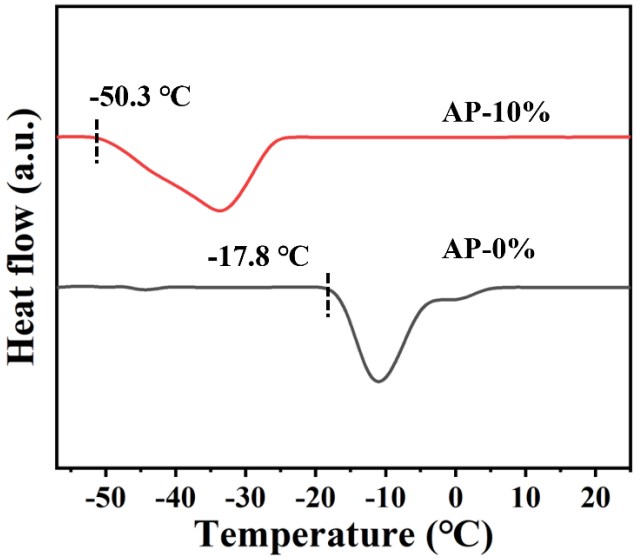


**Figure S3.** DSC curves of AP-0% and AP-10% electrolytes.

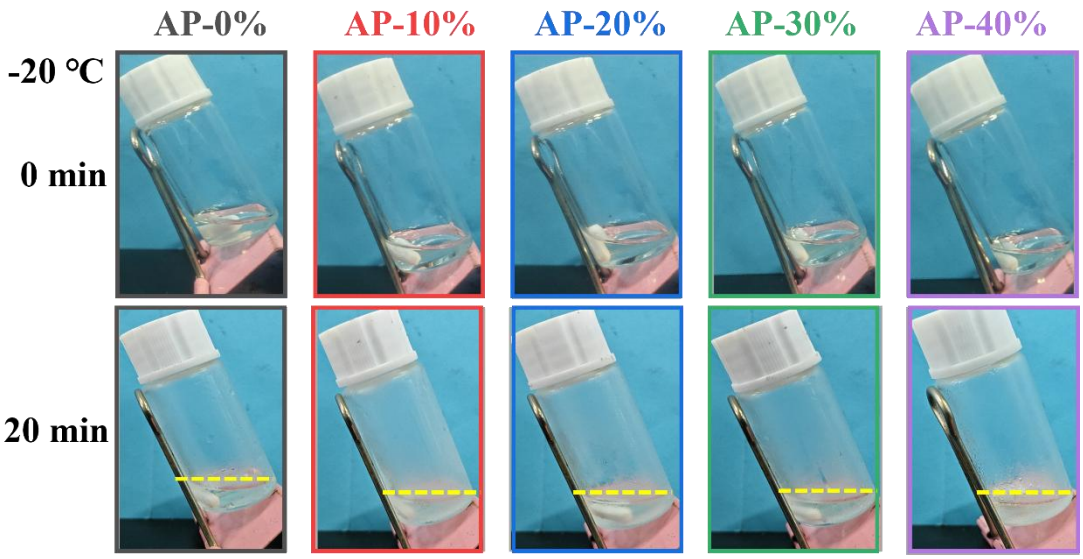


**Figure S4.** Antifreeze performance tests of different electrolytes at -20 °C.

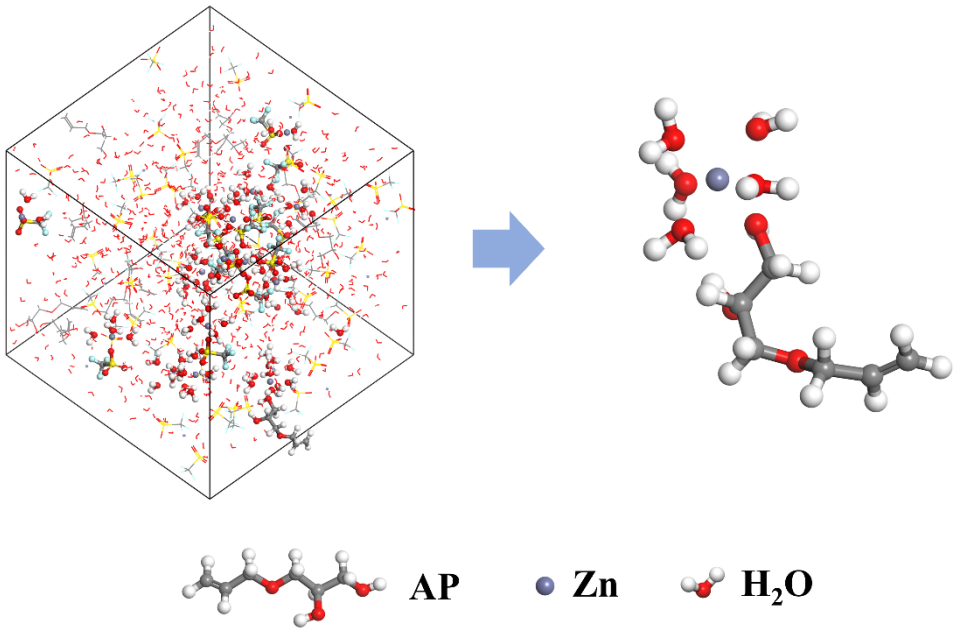


**Figure S5.** 3D snapshots of AP-10% from MD simulations and Solvation structure of $Zn^{2+}$ in AP-10%.

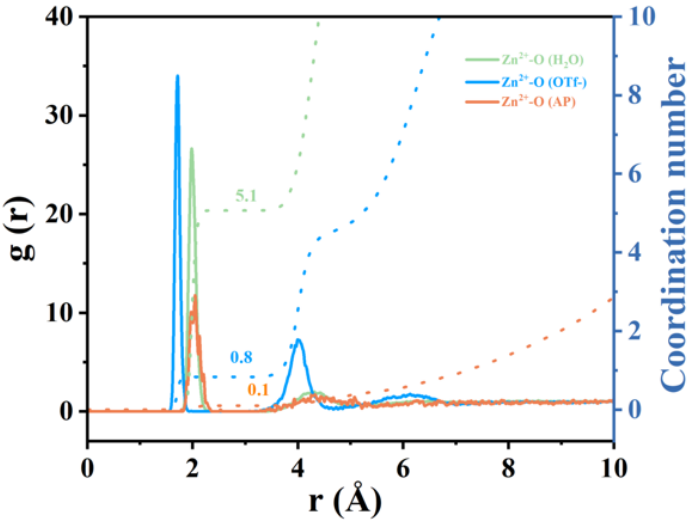


**Figure S6.** Radial distribution function (RDF) and coordination number of $Zn^{2+}$ obtained from MD simulations of AP-10%.

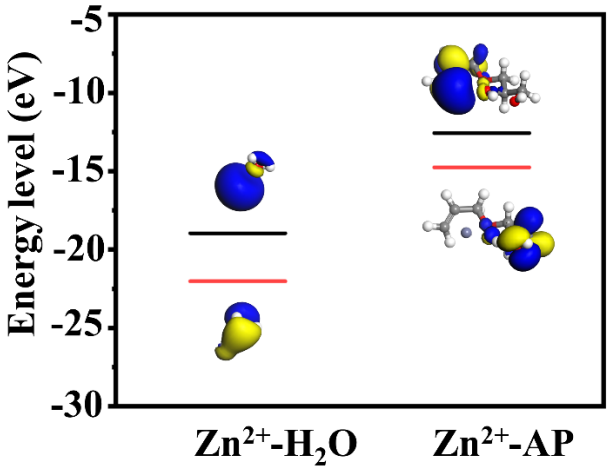


**Figure S7.** The HOMO-LUMO energy gap between Zn-$H_2O$ and Zn-AP.

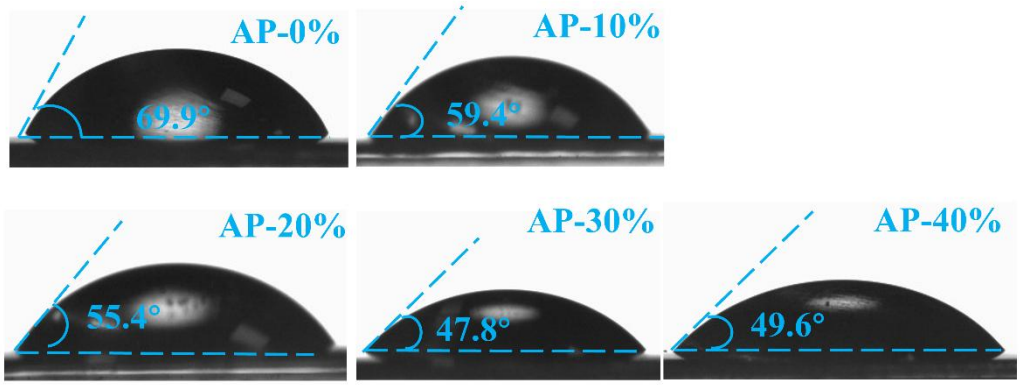


**Figure S8.** Schematic illustration of contact angles for various electrolytes on Zn foil.

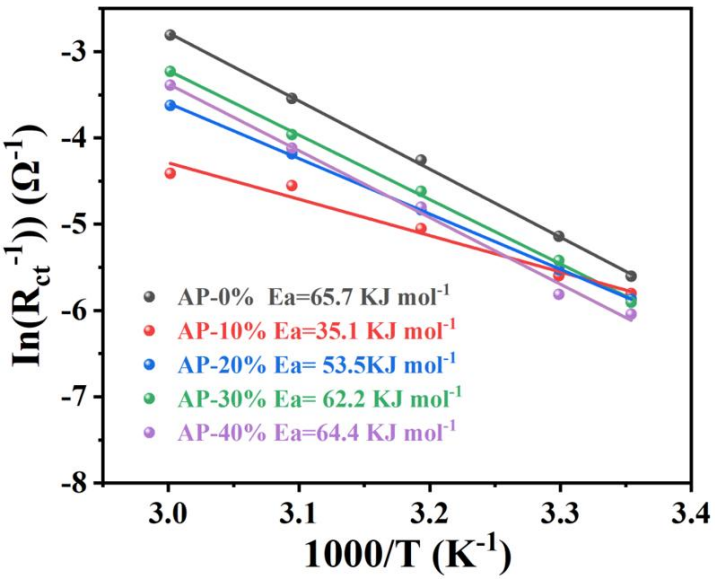


**Figure S9.** Activation energy of different electrolytes.

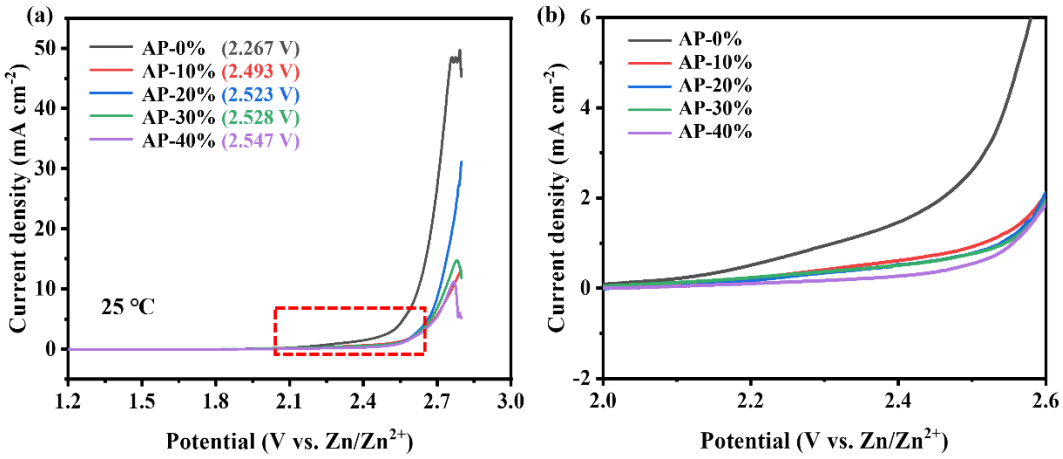


**Figure S10.** OER curves for different electrolytes.

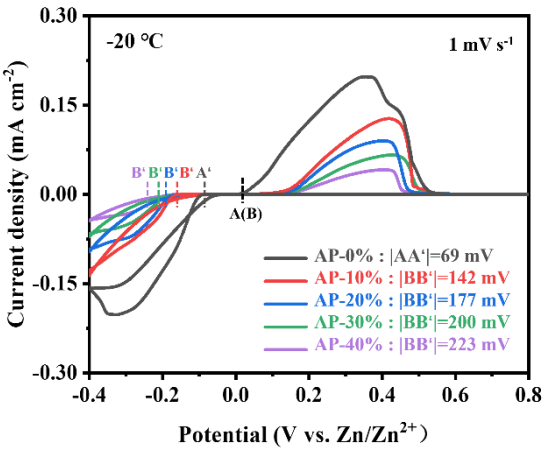


**Figure S11.** CV curves for zinc nucleation at -20 °C.

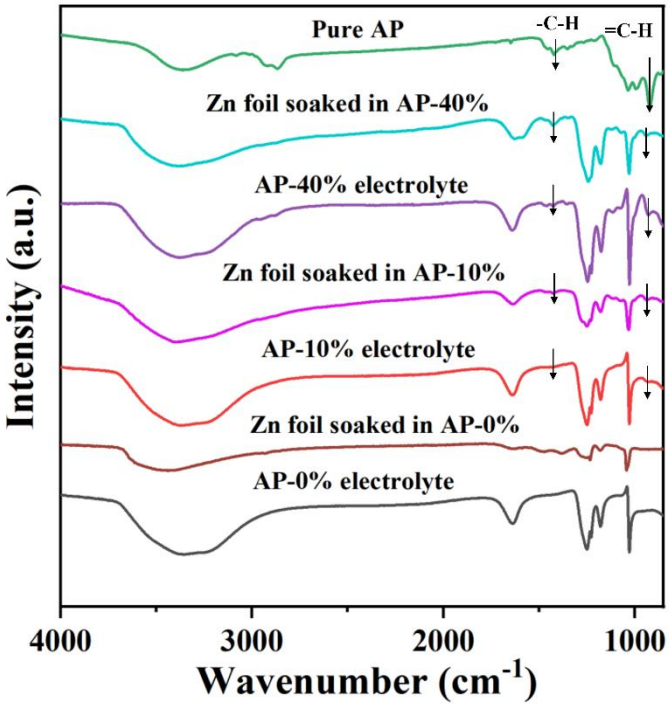


**Figure S12.** FT-IR spectra of pure AP, AP-0%/10%/40% electrolytes, and Zn foils after 3-day soaking in the respective electrolytes (washed and dried).

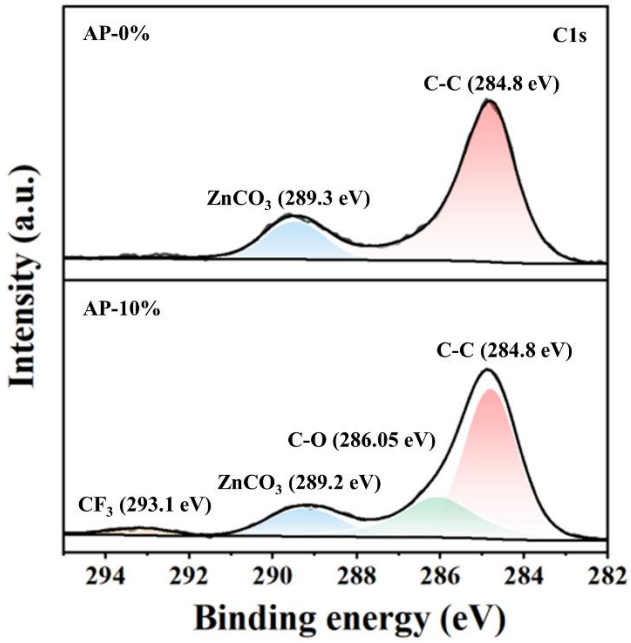


**Figure S13.** XPS of the Zn anode in AP after 100 h cycling.

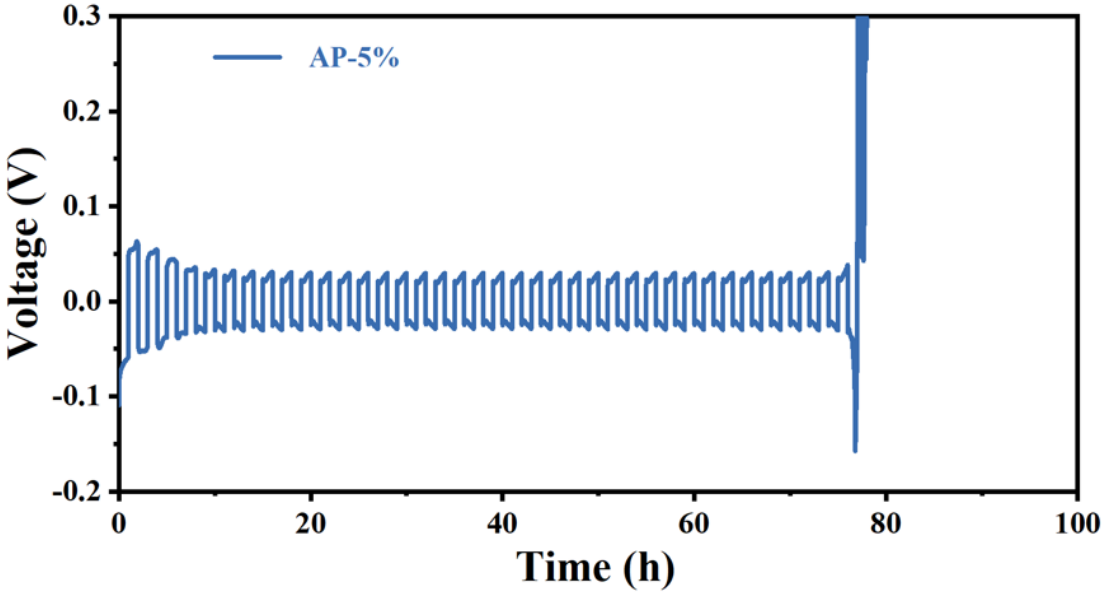


**Figure S14.** Galvanostatic cycling stability of Zn||Zn symmetric cells assembled with AP-5% electrolyte at 1.0 mA $cm^{-2}$/1.0 mAh $cm^{-2}$.

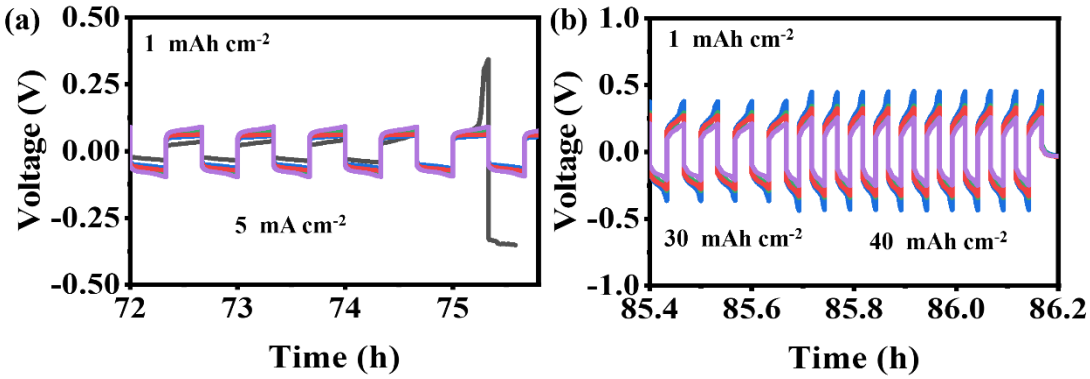


**Figure S15.** Magnified view of the limiting current density of different electrolytes at 25 °C.

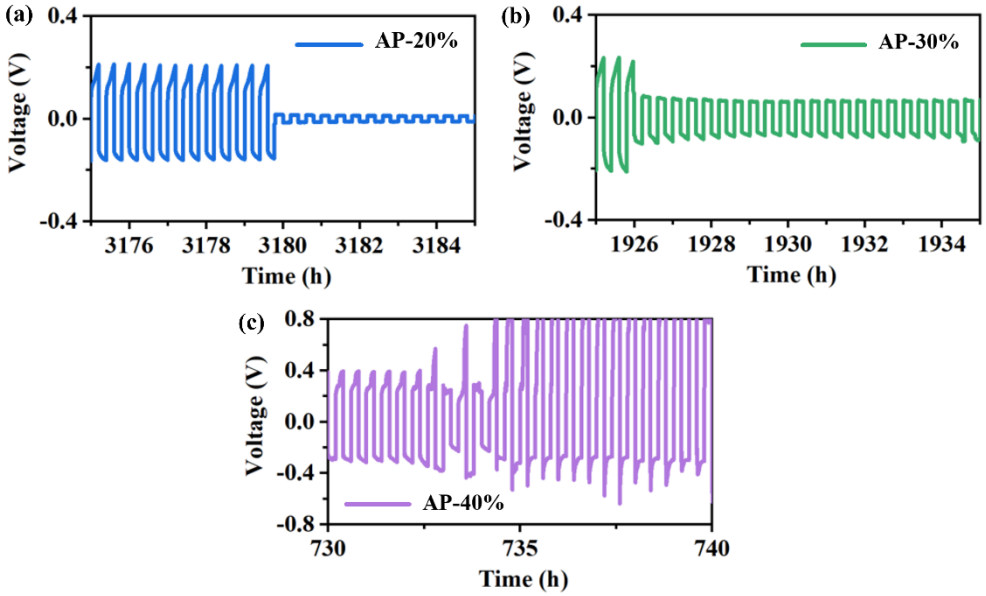


**Figure S16.** Voltage-time curves of different electrolytes.

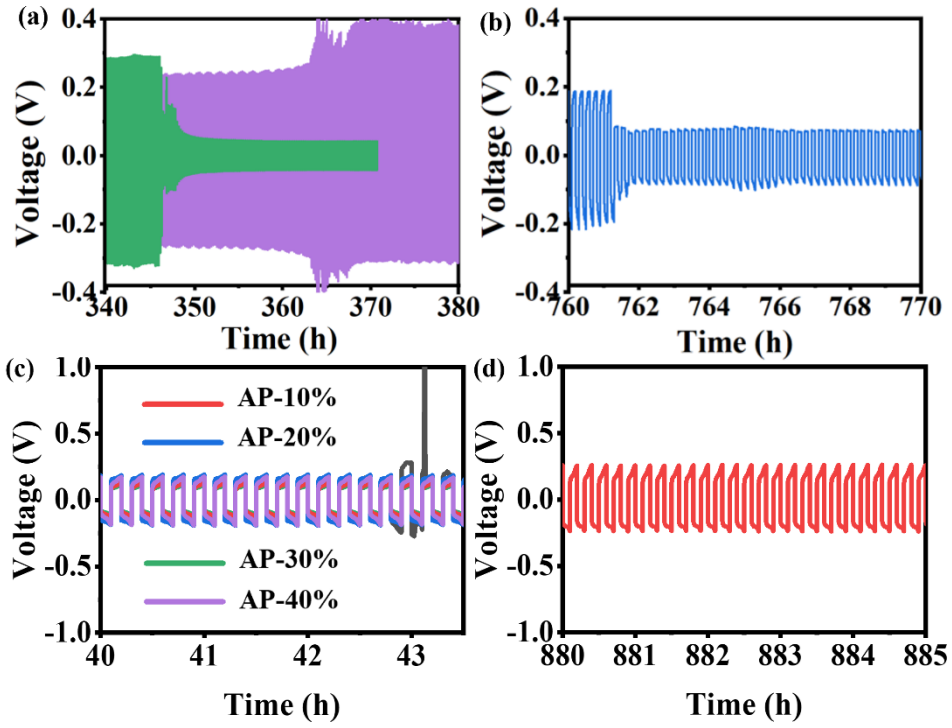


**Figure S17.** Voltage-time curves of different electrolytes.

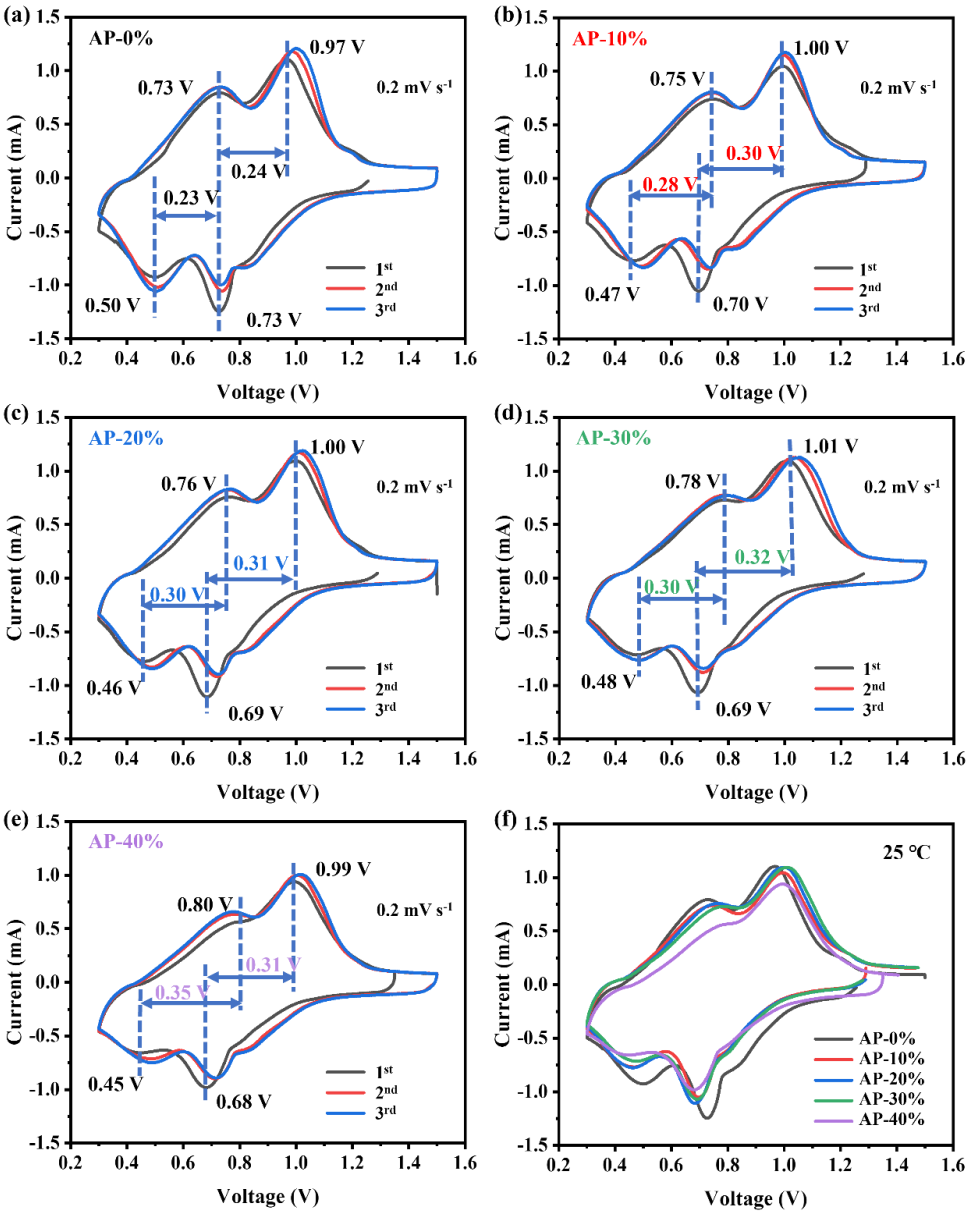


**Figure S18.** CV curves at 0.2 mV $s^{-1}$ employing different electrolytes.

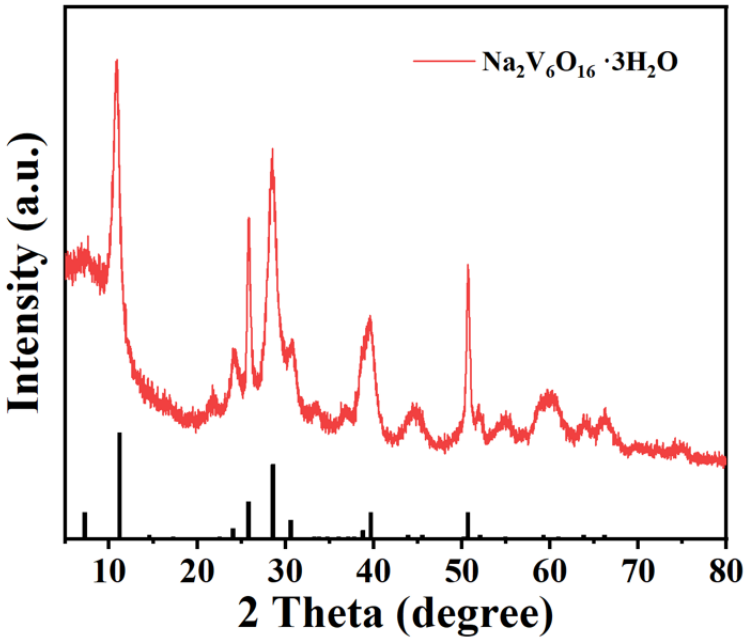


**Figure S19.** The XRD patterns of $Na_2V_6O_{16}·3H_2O$.

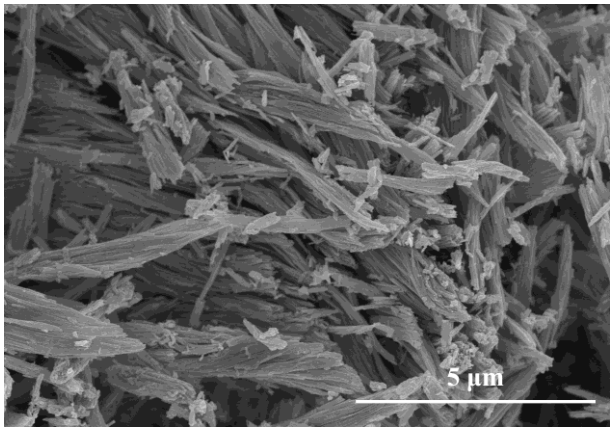


**Figure S20.** The morphology of $Na_2V_6O_{16}\cdot 3H_2O$ by the SEM test.

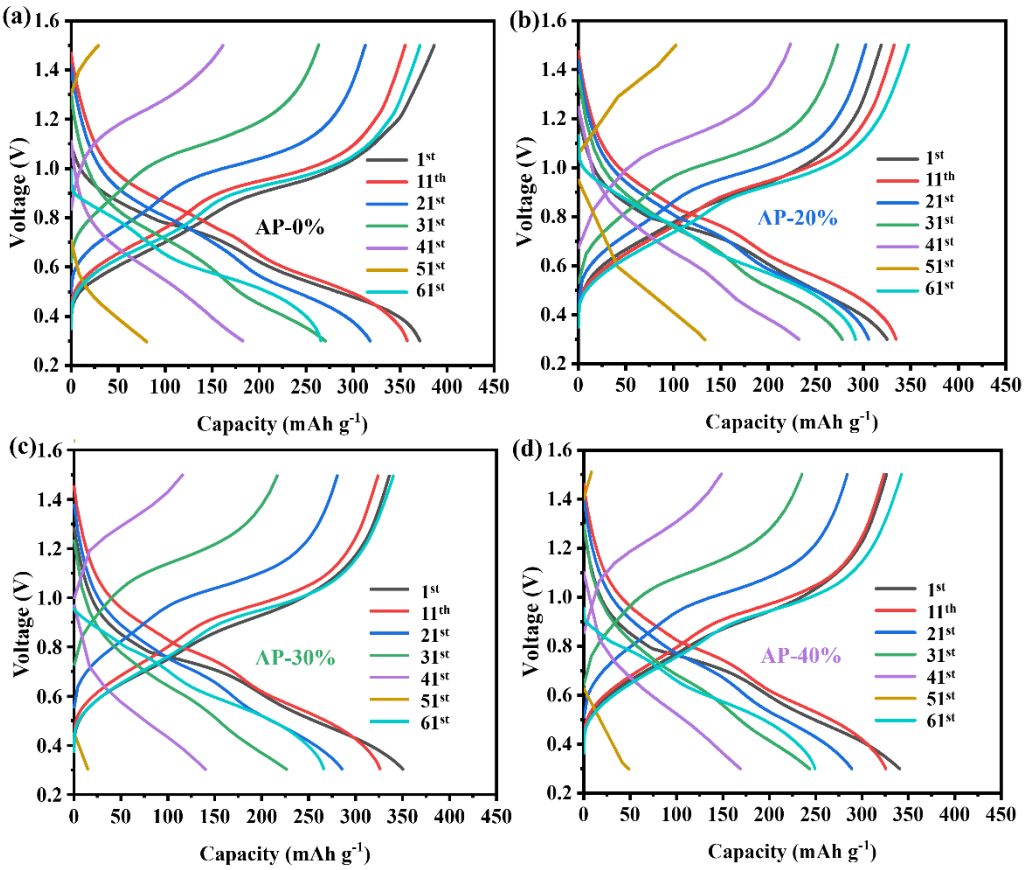


**Figure S21.** GCD profiles at various current densities of different electrolytes at 25 °C.

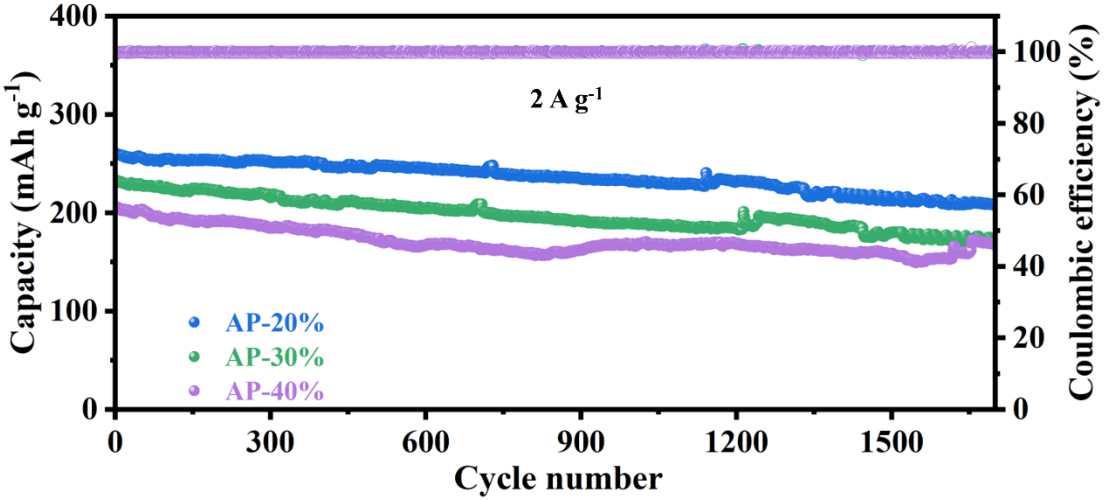


**Figure S22.** Long-term cycling stability at 2.0 A $g^{-1}$.

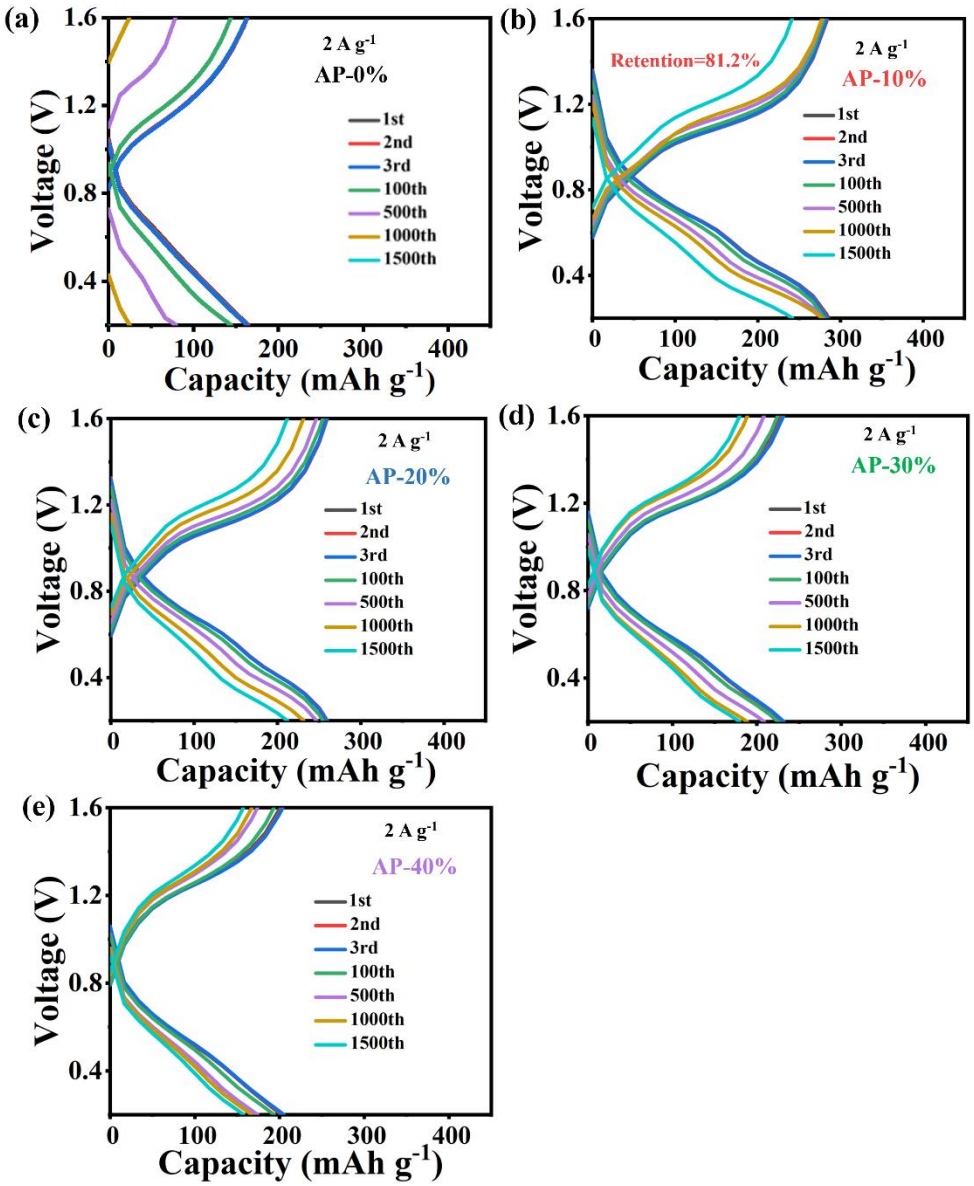


**Figure S23.** The charge/discharge curve of different electrolytes at 2 A $g^{-1}$.

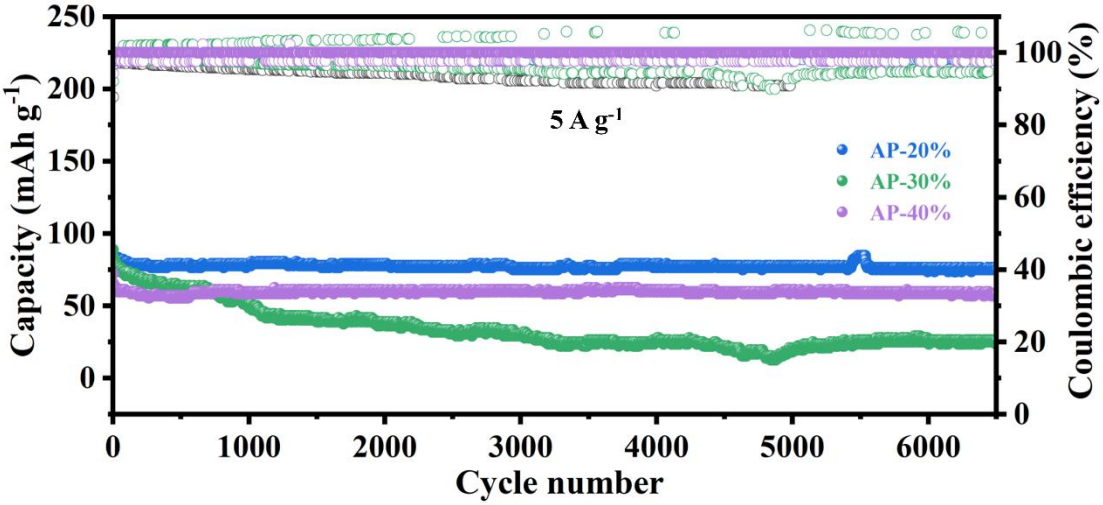


**Figure S24.** Long-term cycling stability at 5.0 A $g^{-1}$.

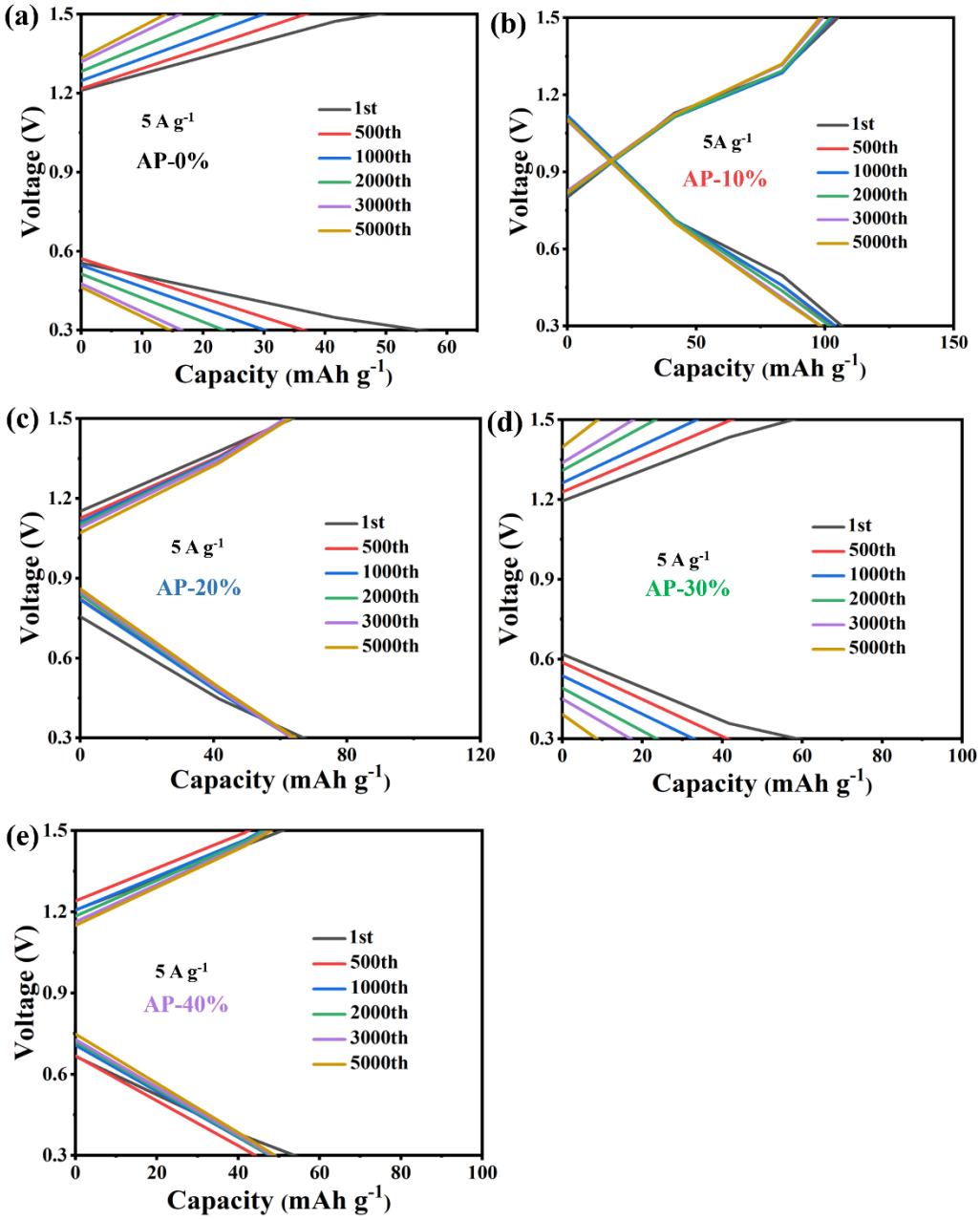


**Figure S25.** The charge/discharge curve of different electrolytes at 5 A $g^{-1}$.

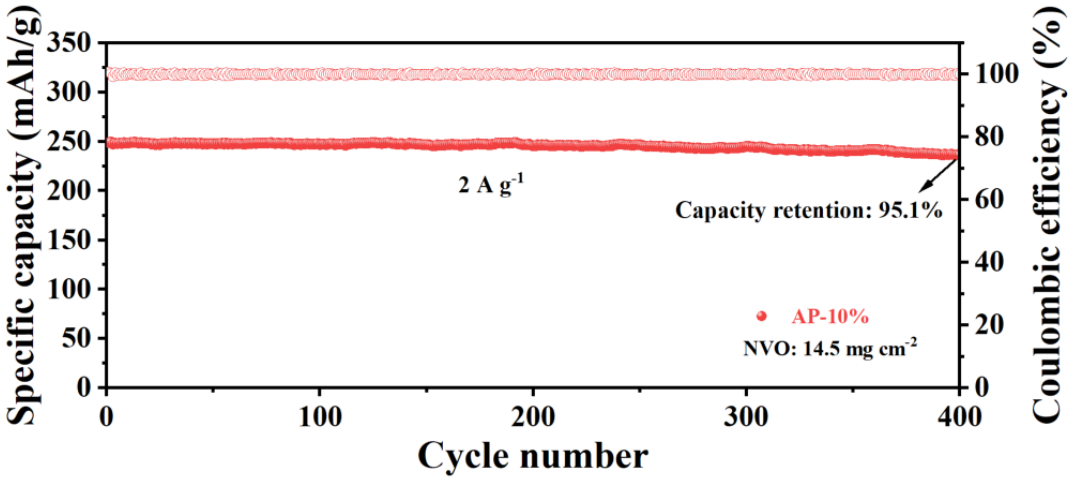


**Figure S26.** Long-term cycling stability of high-loading cathode batteries assembled with AP-10% electrolyte at 2.0 A $g^{-1}$.

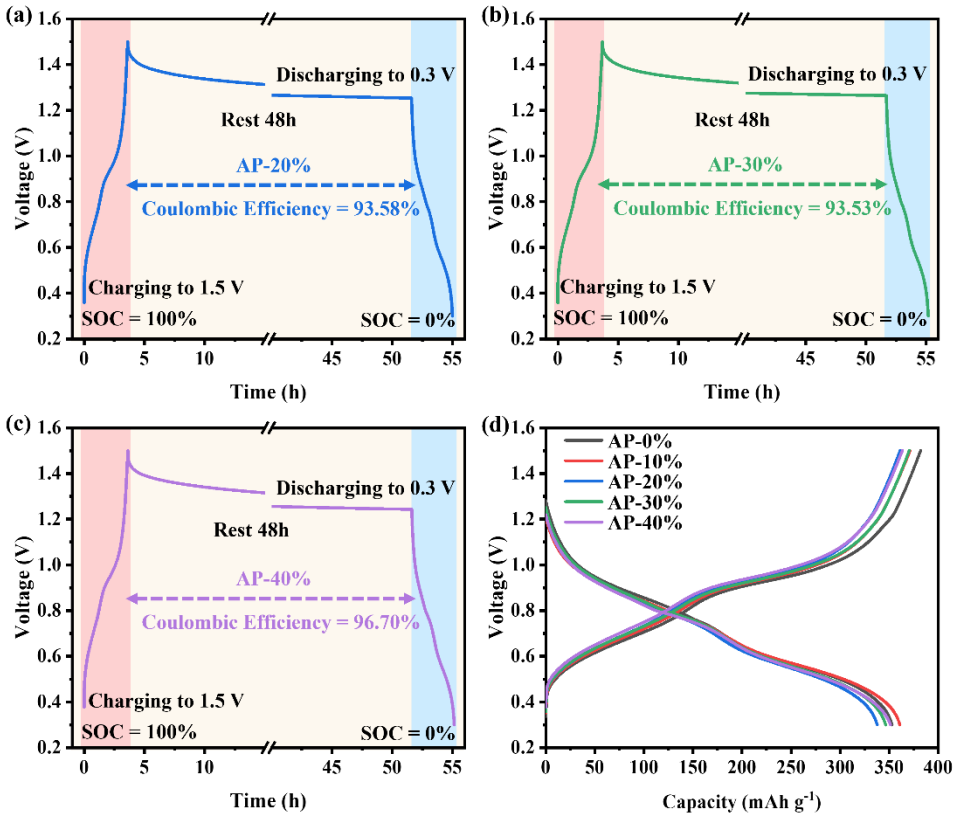


**Figure S27.** Self-discharge behavior of cells with other electrolytes and the charge/discharge curves.

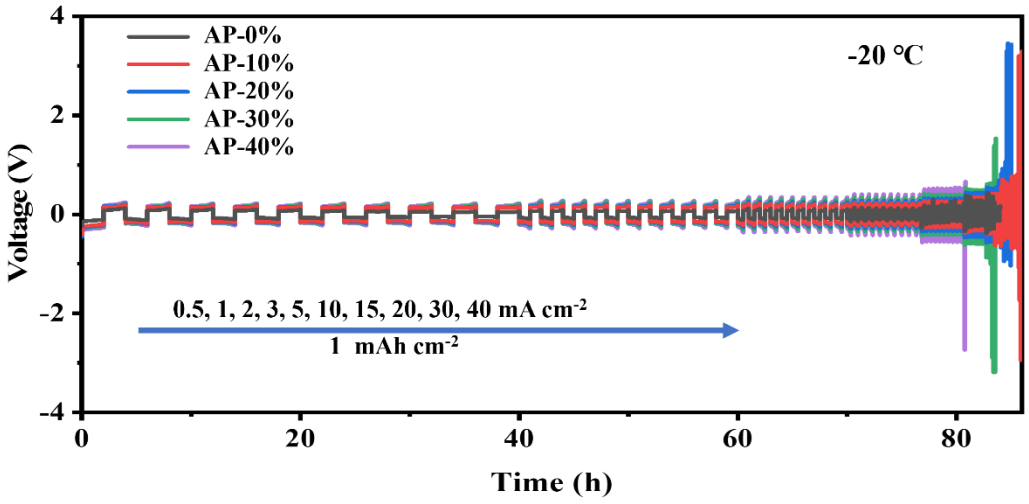


**Figure S28.** The limiting current density of different electrolytes at -20 °C.

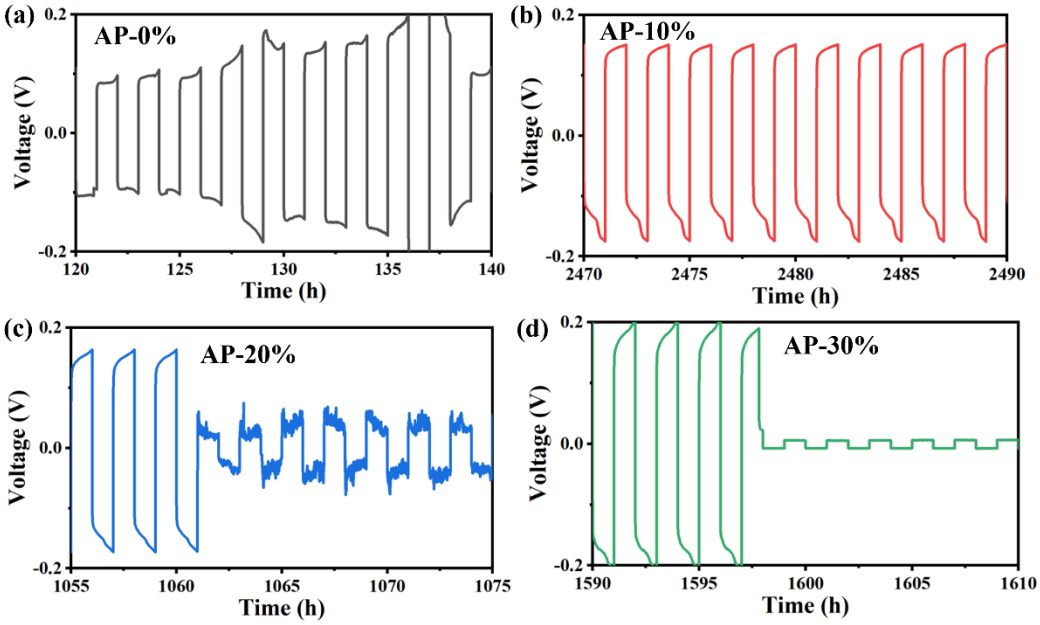


**Figure S29.** Voltage-time curves of different electrolytes.

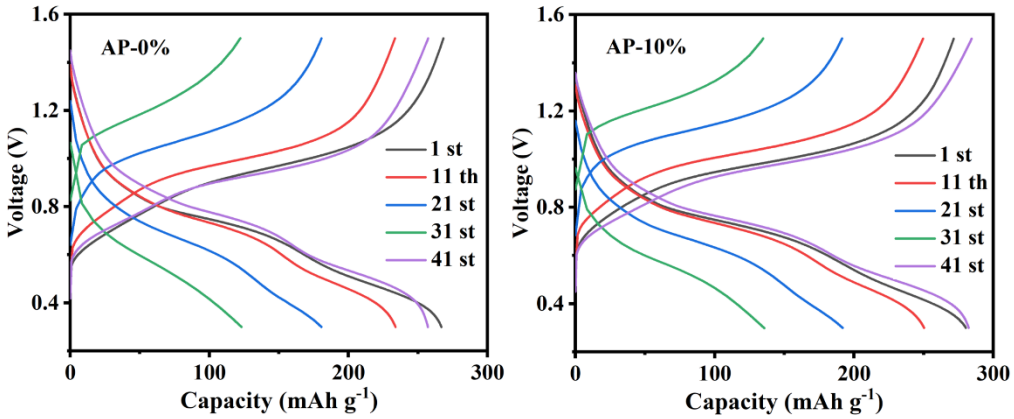


**Figure S30.** GCD curves at -20 °C across varied C-rates.

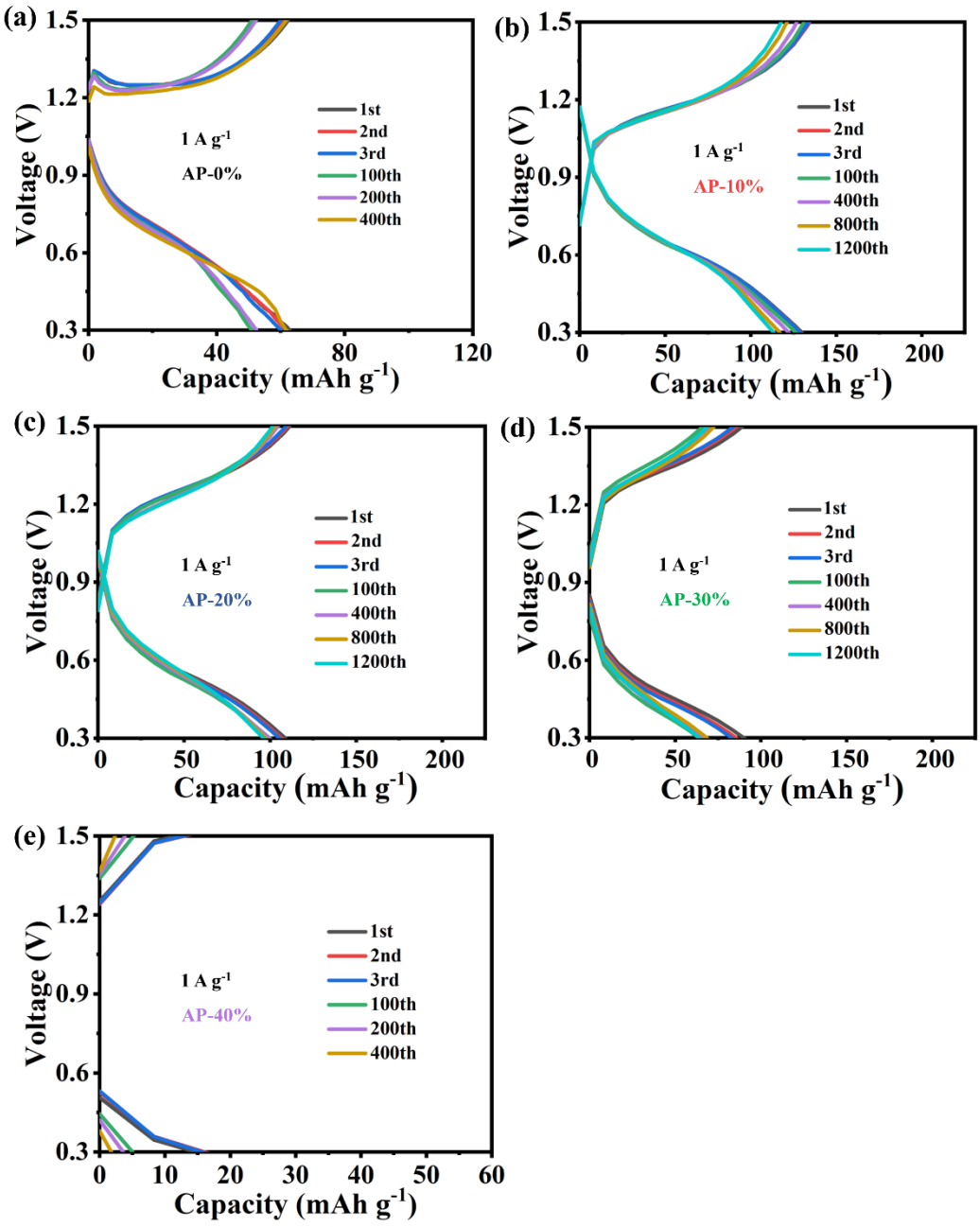


**Figure S31.** The charge/discharge curve of different electrolytes at 1 A $g^{-1}$.

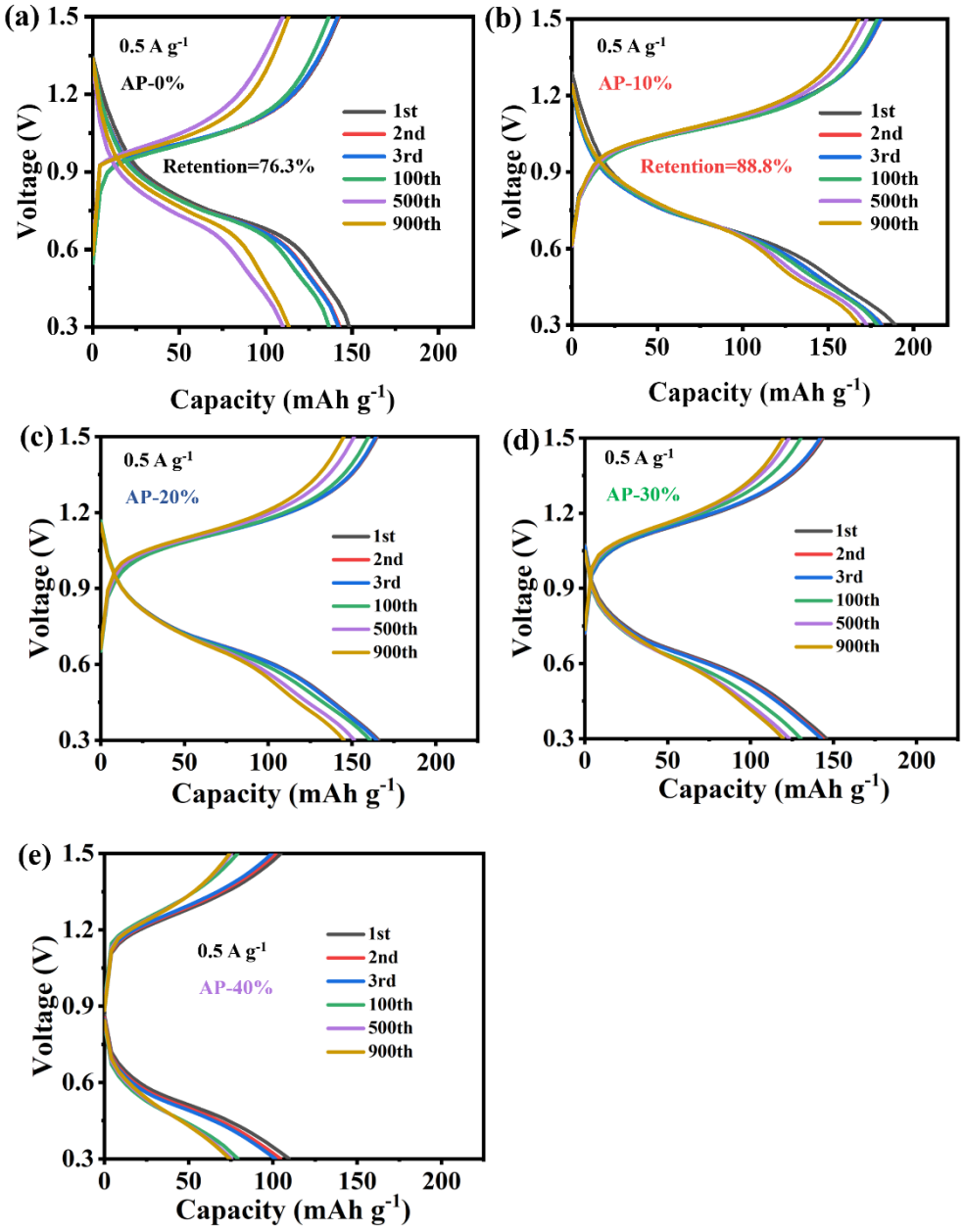


**Figure S32.** The charge/discharge curve of different electrolytes at 0.5 A $g^{-1}$.

**Table S1.** Tafel test values for different ratios of electrolytes.

| Sample | Current density | Potential |
|---|---|---|
| AP-0% | 0.093 mA $cm^{-2}$ | -0.9 V |
| AP-10% | 0.078 mA $cm^{-2}$ | -0.886 V |
| AP-20% | 0.073 mA $cm^{-2}$ | -0.878 V |
| AP-30% | 0.077 mA $cm^{-2}$ | -0.884 V |
| AP-40% | 0.51 mA $cm^{-2}$ | -0.905 V |

**Table S2.** The long-cycle performance comparison of Zn||Zn symmetrical cell assembled with AP-10% and other electrolytes reported so far at an area current less than 5 mA $cm^{-2}$ or area capacity less than 2.95 mAh $cm^{-2}$.

| No | Electrolyte components | Current Density (mA $cm^{-2}$) | Time (h) | Ref. |
|---|---|---|---|---|
| This work | AP-$Zn(OTf)_2$ | 5/1 | 4000 | - |
| 1 | AC-$ZnSO_4$ | 1/1 | 3700 | [61] |
| 2 | SY-$ZnSO_4$ | 2/1 | 1800 | [49] |
| 3 | DP-$Zn(OTf)_2$ | 0.5/0.5 | 3800 | [48] |
| 4 | IS-$Zn(OTf)_2$ | 2.95/2.95 | 400 | [47] |
| 5 | 2H13P-$ZnSO_4$ | 2.5/2.5 | 2200 | [46] |
| 6 | Tris-$ZnSO_4$ | 3/1 | 2600 | [45] |
| 7 | CPME-$Zn(OTf)_2$ | 2/2 | 2400 | [44] |
| 8 | N, S-CDs-$ZnSO_4$ | 1/1 | 1450 | [54] |
| 9 | L-Cys-EG-$ZnSO_4$ | 1/1 | 760 | [60] |
| This work | AP-$Zn(OTf)_2$ | 1/1 | 4500 | - |
| 10 | SAA-$ZnSO_4$ | 1/1 | 3400 | [59] |
| 11 | THF-$Zn(OTf)_2$ | 1/1 | 2800 | [55] |
| 12 | POT-$Zn(OTf)_2$ | 1/1 | 2000 | [57] |
| 13 | DA-$ZnSO_4$ | 2/1 | 1000 | [53] |
| 14 | LA-$ZnSO_4$ | 1/1 | 2300 | [52] |
| 15 | [BMIM]$PF_6$-$ZnSO_4$ | 1/1 | 800 | [50] |
| 16 | NMS-$ZnSO_4$ | 1/1 | 2300 | [58] |
| 17 | PVEMA-$Zn(OTf)_2$ | 1/1 | 2900 | [56] |
| 18 | PM-$Zn(OTf)_2$ | 1/1 | 1700 | [51] |

## Reference for Supplementary Information


[1] Lee C, Yang W, Parr R. Development of the Colle-Salvetti correlation-energy formula into a functional of the electron density. Phys Rev B, 1988, 37, 785-789

[2] Becke A. Density-functional thermochemistry. III. The role of exact exchange. J Chem Phys, 1993, 98, 5648-5652

[3] Grimme S, Antony J, Ehrlich S, et al. A consistent and accurate ab initio parametrization of density functional dispersion correction (DFT-D) for the 94 elements H-Pu. J Chem Phys, 2010, 132, 154104